Empirical Propagation Performance Evaluation of LoRa for Indoor Environment

Salaheddin Hosseinzadeh, Hadi Larijani, Krystyna
Curtis, Andrew Wixted
School of Engineering & Built Environment
Glasgow Caledonian University
Glasgow, UK
salaheddin.hosseinzadeh@gmail.com, h.larijani@gcu.ac.uk,
krystyna.curtis@gcu.ac.uk, andrew.wixted@gcu.ac.uk

Amin Amini
School of Electronics and Computer Engineering
Brunel University
London, UK

Abstract— **Wireless sensors are increasingly being used for smart Buildings. LoRa is a chirp spread spectrum (CSS) technology. Its CSS modulation provides wide bandwidth, increased processing gain and higher receiver sensitivity. Propagation analysis of this long-range low power wireless platform is essential to make it a prevailing technology of choice for IoT. This paper empirically evaluates the indoor propagation performance of LoRa. The practical measurements were critically analyzed against four propagation models; ITU site generic, log-distance, multi-wall and 3D ray tracing. Data was collected in the Hanover building at Glasgow Caledonian University using the LoRa transceivers. The aims of this research were (1) to assess the indoor propagation performance of LoRa technology and (2) to identify the model that best describes the indoor propagation of LoRa. The study concluded that multi-wall has the best overall performance amongst the models. This research work will facilitate the link budget design, network implementation and coverage diagnosis in similar indoor scenarios.**

Keywords—Internet of Things (IoT); LoRa propagation; LPWAN; indoor propagation estimation; ITU model; log-distance model; Motley-Keenan model; COST231 model; 3D ray-tracing model

I. INTRODUCTION

Since one of the main challenges in the realization of wireless sensor network systems is to minimize the node deployment and maintenance cost, having the knowledge of the propagation can be a key for designing an efficient, reliable and cost-effective network. LoRa and Sigfox are two of the long range low-power wireless solutions for IoT, with LoRa being an open standard system and freely available. A survey of available low-power wide area network (LPWAN) devices is carried out by Reza. et al [1].

LoRa is a relatively new ISM band (33, 868, 915 MHz) LPWAN technology that is intended for battery-operated wireless devices. LoRa satisfies the IoT requirements such as secure bi-directional communication, mobility and localization services. The standard can also provide seamless interoperability between smart devices. Therefore, providing freedom to the users, developers and businesses to take advantage of IoT [2][3].

In addition to its low-power consumption, LoRa is also resistant to multipath, owing to its proprietary spread spectrum method based on CSS modulation [5][6][7]. Therefore, making it a favorable choice for indoor environments where multipath fading, due to reflections, is the dominant phenomenon. Further LoRa technological information is presented in [4].

Due to the prevalence of 2.5 and 5 GHz wireless systems, there has been a significant research, especially in the field of channel modeling and propagation in these frequencies. Similarly, since the 900 MHz band is used in mobile communications, a majority of the measurements have been carried out for cellular technology to investigate the propagation in macro-cells and into buildings. Therefore, leaving a gap for the recently introduced LPWAN technologies.

To the best of our knowledge, the only related published research is carried out by Juha.et.al [7]; where authors investigated coverage range of LoRa in the city of Oulu, Finland for two scenarios: a) in the city b) on the sea. Authors compared the packet loss ratio and signal strength against the coverage range by logging the signal strength indicator (RSSI) from the LoRa, mainly under a line of sight (LOS) condition. This is done while the transmitter kept stationary and the receiver moved at a speed ranging from 40 to 100 km/h. Authors compared the real-world measurements against the log-distance model to derive the path loss exponent, and therefore evaluating the propagation performance of LoRa in both scenarios.

The main contributions of this paper are:

- Collection of real-world measurements on a large campus building using LoRa transceivers to analyze and evaluate its indoor propagation performance.

- Investigation of the propagation characteristics and advantages of the LoRa for indoor scenarios by comparing the empirical and theoretical indoor propagation results.

- Identifying the model that best estimates the indoor propagation of LoRa with four propagation models. These propagation models are ITU indoor, log-distance

26

path loss with shadowing, multi-wall model [8] and 3D ray tracing.

- <mark>Analysis of propagation characteristics of the Hanover building for sensor network planning and future propagation studies.</mark>

This paper is arranged as follows. In section II the investigated models are described briefly. Section III explains the development of the models in MATLAB. Section IV explains the practical measurement setup and details. Section V presents the analysis of the measurement and its comparison with models. Finally, section VI concludes the research.

II. PROPAGATION MODELS

This section introduces the models that are used to estimate the signal propagation. Selected models are covering different levels of complexity, and are commonly used to estimate the indoor propagation.

A. ITU & Log-distance

ITU non-deterministic indoor propagation recommendation estimates the path loss inside a building such a room or closed area. <mark>The model is applicable to indoor scenarios with 1 to 3 floors and frequency range of 900 MHz to 5.2 GHz.</mark> ITU model is mathematically expressed in Eq.(1) [9].

$$L = 20 \log f + N \log d + P_f(q) + 28 \qquad (1)$$

Where L is the path loss in dB, f is the frequency in MHz, N is the distance power loss coefficient, q is the number of floors between transmitter and receiver and finally $P_f(q)$ is the floor loss penetration factor, which is 0 for measurements on the same floor. <mark>ITU model is also very similar to the log-distance path loss with shadowing except, the latter attempts to account for the clutter between the transmitter and receiver by an additional term that accounts for the effect of shadowing.</mark>

The model in Eq.(2), is commonly used in the link budget analysis to predict the path attenuation (L) in dB.

$$L = L_0 + 10n \log(d/d_0) + X_\sigma \qquad (2)$$

Where L_0 is the free-space loss (dB) at a reference distance (d_0) of 1 m, n is the path loss exponent, which is derived experimentally, and d is the distance between the transmitter and receiver in meters. X_σ is a Gaussian random variable (in dB) with a mean of zero and standard deviation of σ dB.

B. Multi-wall Model

COST 231 and Motley-Kennan are relatively similar multi-wall models. <mark>In addition to the distance between transceivers, they also require the number of the walls between the transceivers. By assigning certain attenuation factor to each wall, the models account for additional attenuation incurred by the structure. This attenuation is due to the signal impinging the walls to reach the other transceiver.</mark> COST 231 also accounts for the floor attenuation but to avoid overestimating, it rolls off transition losses after a certain number of floors have been impinged [10][11]. Motley-Keenan model and COST 231 (without the floor loss) are presented in Eq.(3).

$$L = L_0 + 20 \log(d) + \sum k_j \alpha_j \qquad (3)$$

Where k_j is the number of panels of type j between the transceivers and α_j is the attenuation factor of the same type of wall.

C. Ray Tracing

Ray tracing is site specific and therefore a more accurate method of estimating the radio signal propagation for indoor environments. Although it is capable of estimating the channel response (path gain and delay spread), it is sophisticated and computationally more demanding than aforementioned models. In 3D ray tracing, the channel impulse response $h(t)$ at a given point is formulated in Eq.(4).

$$h(t) = \sum_{i=1}^{I} \left[\left(\prod_{u=1}^{M_{ri}} \Gamma_{iu}(\theta_{iu}) \times \prod_{v=1}^{M_{pi}} P_{iv}(\theta_{iv}) \right) \frac{1}{r_i} \right.$$
$$\left. \cdot e^{-j\omega\tau_i} \cdot \delta(t - \tau_i) \right] \qquad (4)$$

Where i is the number of rays reaching a particular point, M_{ri} is the number of reflected rays and Γ_{iu} is the reflection coefficient of ray i for wall u, Similarly, P_{iv} is the transmission coefficient of ray i for wall v, and θ_i is the incident angle of the ray i. With r_i being the path length of ray i and $e^{-j\omega\tau_i}$ representing the carrier with time delay of τ_i

III. MODEL IMPLEMENTATION

All the explained propagation models were implemented in MATLAB. For ITU, log-distance and multi-wall models the simulation start by acquiring a 2D blueprint image of the structure. The image PPI (pixel per inch) is then calibrated so that all the walls/panels on the picture represent the actual building dimensions. This is performed by providing the length of a particular wall (meters) to the algorithm and then selecting two end pixels that correspond to that particular wall. Algorithm then calculates the LOS distance between the TX and RX.

<mark>In the case of the multi-wall model, to detect the number of panels between the TX and RX, Bresenham's line algorithm [12] was used with a combination of image processing techniques to find the intersection of a straight line, between RX and TX, and the blueprint image.</mark> This approach was considered to facilitate the structural design, as no 3D model will be required and there is no need to define walls in a vector form database. The 3D ray tracing algorithm, however, requires the building model as a DXF (Drawing Exchange Format) file. Therefore, every finite panel is defined by a set of 4 corners in the Cartesian coordinate and a normal vector, which specifies the orientation of the panels. The 3D ray tracing algorithm then takes advantage of MATLAB's matrix operations and linear algebra as it was implemented using geometrical optics model similar to [13][14][15][16][17] [18]. To predict the received power, further details are added to the simulation such as the transceiver parameters (efficiency, VSWR and transmitting power), ray's angle of departure (from transmitting antenna) and angle of arrival (to the receiving antenna) and the directivity of the antennas.

IV. PRACTICAL MEASUREMENT SETUP

In this section, the measurement setup is explained in details. Real-life measurements were carried out at Glasgow Caledonian university student association (Hanover building) with dimensions of 36 × 26.5 m. The blueprint of different floors are depicted in Fig.1 and Fig.2 with 3D ray tracing propagation map, measurement locations and the transmitter location imposed on top.
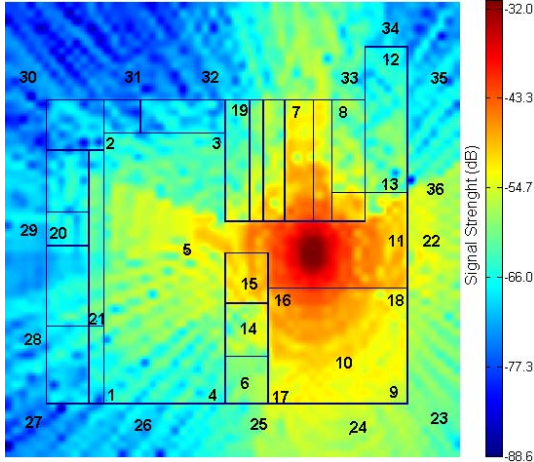

Fig. 1. Ground floor 3D ray tracing signal strength propagation map. TX and measurement locations 1-36.
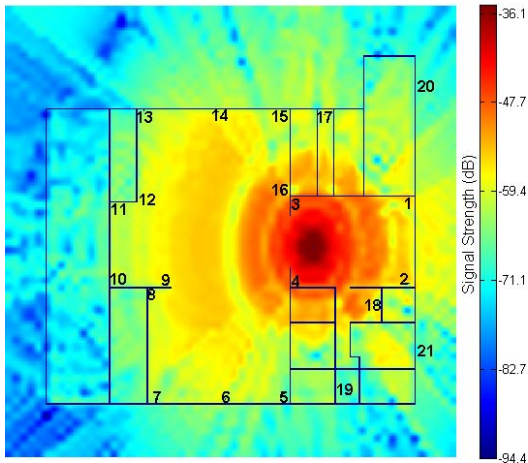

Fig. 2. First floor 3D ray tracing signal strength propagation map. TX and measurement locations 1-21.

During the measurements the transmitter was placed at a fixed position inside the building while the receiver moved to different locations within and around the building. The transmitter and receiver are kept at a fixed height of 1.5 m during the measurements. The signal strength measurements at each location within the different floors are provided in Fig.3 and Fig.4.

SX1272 transmitter and receiver are connected to an Arduino micro-controller and a Raspberry pi respectively, as shown in Fig.5. The transmitter sends a packet every 2 seconds on channel 10 (865.20 MHz) with a bandwidth of 125 KHz at 14 dBm. The packets also include a sequential number, in order

to identify the packet loss. The transmitter is configured with the maximum spreading factor of 12, and error correction code of 4/5. Receiver appends the RSSI to the received message and logs it in a text file on the Raspberry pi. 200 samples collected at each position and RSSI averaged to determine the signal strength at each position. Half wavelength dipole antennas are used for both devices with VSWR < 2, the peak gain of 2dB and linear vertical
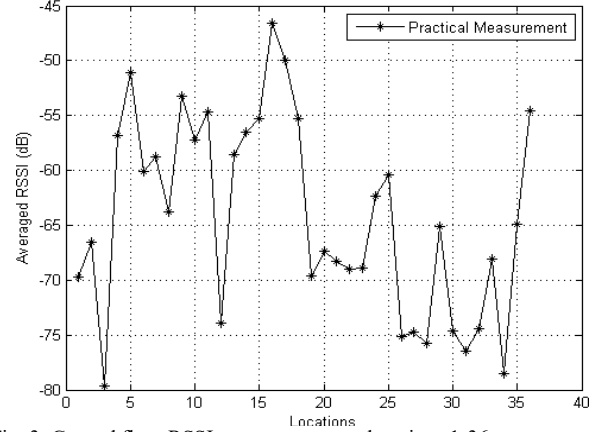

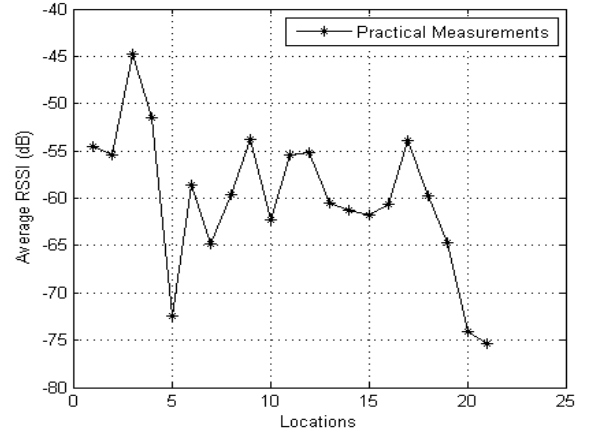Fig. 3. Ground floor RSSI measurements at locations 1-36.

Fig. 4. First floor RSSI measurements at locations 1-21.

Fig.5. Transmitter and receiver hardware.

polarization.

V. PROPAGATION ANALYSIS

To evaluate the indoor propagation characteristics of LoRa, first parameters of individual models are optimized for each floor. This is carried out by minimizing the mean square error

28

(MSE) of estimations according to the measurements. Later using the optimized parameters in Table I the signal strength maps are produced for each model, 3D ray tracing maps are depicted in Fig.1 and Fig.2 as an instance.

To compare and benchmark the accuracy of each model, the MSE of the estimated RSSI are tabulated in Table II for each floor. For each location, the estimated and measured signal strength values are depicted for every individual model and both floors in Fig.6 and Fig.7.
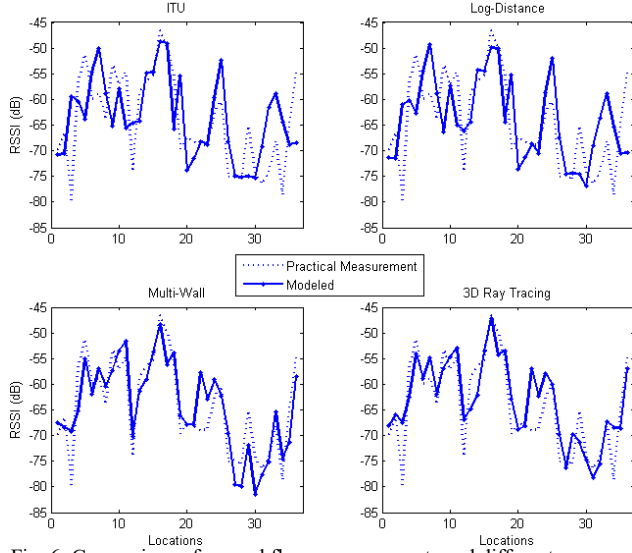

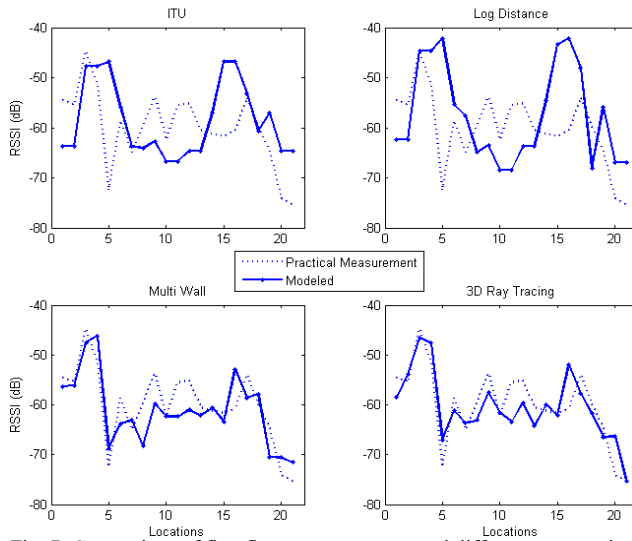Fig. 6: Comparison of ground floor measurements and different propagation models.

Fig. 7: Comparison of first floor measurements and different propagation models.

A. ITU & Log-distance Models Analysiss

Empirical RSSI measurements on the ground floor are compared with the ITU and log-distance estimations. As explained before, the model parameters are derived using MMSE estimator. For ground floor and first floor, MSE of ITU converged to 67 and 90 dB, resulting in the distance power loss coefficients (N) of 27.8 and 25.5 respectively. Similarly, for the

ground floor, MSE of log-distance converged to 69.5 and 87 dB, resulting in the path loss exponents (n) of 2.75 and 2.7 respectively.

B. Multi-wall Model Analysis

Propagation parameters of the multi-wall model are the walls attenuation factor, many of which are reported in [19][20][9] for various structural materials. The reported values are used as the initializing value of optimization and further adjusted to minimize the MSE to 22 & 20 dB for ground floor and first floor respectively. Based on visual inspection, and to facilitate the optimization, walls are divided into four homogeneous types: glass, concrete, brick, plasterboard, indexed with j = 1, 2, 3 and 4 respectively. Derived values of α for all the four types of walls are tabulated in Table I for both, ground and first floor, scenarios.

TABLE I. PROPAGATION MODEL PARAMETERS FOR ALL 4 MODELS AND BOTH SCENARIOS (GROUND AND FIRST FLOOR)

Model	Parameters	Ground floor	First floor
ITU	N	27.8	25.5
log-distance	n	2.75	2.5
	σ	1.3	1
multi-wall	α_1	1.53	1.53
	α_2	4	4
	α_3	3.2	3.2
	α_4	3	3
ray tracing	ε_{r_1}	2.2	2.2
	ε_{r_2}	6.5	6.5
	ε_{r_3}	5.5	5.5
	ε_{r_4}	3.5	5
	ε_{r_5}	8.5	3.5
	ε_{r_6}	13	4

TABLE II. MSE FOR ALL 4 MODELS.

MSE (dB)	Ground floor	First floor
ITU	67	90
log-distance	69.5	87
multi-wall	22	20
ray tracing	22	14

C. 3D Ray Tracing

A 3D model of the environment is used to determine the signal propagation using ray tracing method for both scenarios. The small size windows and doors lying in the same plane as a wall are not included in the 3D model as they are assumed to be the same material as the wall. This approximation is made to reduce the number of reflecting panels and as a result accelerate the 3D ray tracing. Ground floor and first floor were modeled with approximately 40 panels (including ceiling and floor). For the same reason, furniture, vending machines and similar equipment were omitted in the 3D model. The ray tracing algorithm only accounts for the first and second reflections. As reported previously, considering more than 2 reflection, up to 6, changes the signal strength by only 1 dB, nonetheless, it increases the complexity and execution time exponentially [13].

Unlike the multi-wall model, which has fixed attenuation factors for the walls, in ray tracing a fixed effective permittivity is assigned to each wall. However, transmission and reflection

coefficients change according to the changes in the angle of the incident of the ray. The reflection and transmission coefficients are then determined according to the associated relative permittivity (ε_r) of the constructing material. Both Γ and P are calculated by Fresnel equations, taking into account the incident angle and polarization of the beam. Due to the vertical polarization of the transmitting antenna, TE coefficients are used for the walls and TM for the ceiling and the ground planes. Similarly, the four types of walls are considered with relative permittivities ($\varepsilon_{r=1,...,4}$), ceiling (ε_5) and the ground (ε_6); thus a total of 6 different relative permittivities. These parameters are tabulated in Table I after optimization, which yielded the MSE of 22 & 14 dB for the ground floor and first floor respectively.

VI. CONCLUSION AND RESULTS

According to the ITU recommendation report, power loss coefficient (N) is in the range of 20 to 33 for commercial and office areas. This investigated parameter ($N \approx 26$) of the ITU model is in the middle of the same range. Therefore, characterizing the Hanover building as hybrid structure, standing between commercial and office environments. For log-distance model the path loss exponent (n) emerged as nearly one-tenth of distance power loss ($n \approx 0.1N$), due to the similarity of the two models.

In spite of optimizing the propagation models independently for ground floor and first floor, the effective attenuation and permittivity coefficients of both scenarios are similar, except ε_4 which is slightly different. This further validates the assumption of having four main types of different walls in the building. The considerable discrepancy of ε_5 and ε_6 between the two scenarios was expected as the material of ceiling and floor planes are different. Also, the obtained coefficients are in agreement with previously reported values. However, attenuation and permittivity coefficients of glass walls/panels are in their lower range.

Although the non-deterministic models (ITU, and log-distance) correctly characterized the propagation environment as semi-commercial, it is apparent that these two models are lacking accuracy, compared to ray tracing or multi-wall models. ITU and the log-distance predictions resulted in higher MSE compared to that of a multi-wall or ray tracing. ITU and log-distance are good choices when there is no model of the structure, modeling of the environment is difficult and the computation and complexity of a 3D ray tracing are cumbersome.

Furthermore, in this study the 3D ray tracing resulted in an estimation similar to that of the multi-wall model without requiring a 3D model of the structure or demanding computational power. The 3D ray tracing generated the best results, however, this advantage is almost negligible over multi-wall model which offers a greater simplicity. This similarity in estimations can be due to the LoRa's resistance to multi-path, making the 3D ray tracing not as effective. 3D ray tracing is advantageous if the small scale fading estimations are of interest, however, that requires a sampling interval of less than half-wavelength.

In conclusion, the multi-wall model is considered as the best candidate for the indoor LoRa scenario, as a result of retaining an acceptable trade-off between the complexity and accuracy. Derived attenuation and permittivity factors from multi-wall and 3D ray tracing models, further clarifies that the real-world obtainable performance of this LPWAN technology is foreseeable with classical propagation models.

Despite the RSSI reaching -80 dB, no packet loss was observed during the measurements at any of the locations. In few locations on the ground floor, there is a considerable difference between the measurements and estimations. This is due to the LOS clutter between TX and RX, for instance in locations 3 and 22 (Fig.3). In the location 3, the direct path was obstructed by the vending machines, causing additional attenuation. Measurement location 22, was located behind a metallic fire exit gate to observe its impact on propagation. Compared to the simulation there is about 10 dB attenuation as a result of the metallic gate. This gate is, however, ignored in the modeling as it does not have a considerable surface area compared to the walls.

Currently Glasgow has a LoRa & LoRaWAN set up covering about 12 Km^2. The network is mainly used for air pollution and transport systems monitoring. A future expansion of this research will be to investigate the LoRa propagation in the city of Glasgow, which has metropolitan, urban, extra-urban and older historic areas.

REFERENCES

[1] U. Raza, P. Kulkarni, and M. Sooriyabandara, "Low Power Wide Area Networks: A Survey," *arXiv preprint arXiv:1606.07360,* 2016.

[2] "LoRa Alliance," [Online]. Available: https://www.lora-alliance.org/.

[3] A. Augustin, J. Yi, T. Clausen, W. M. Townsley, "A Study of LoRa: Long Range & Low Power Networks for the Internet of Things," *Sensors,* vol. 16, no. 9, p. 1466, 2016.

[4] K. Mikhaylov, J. Petaejaejaervi, T. Haenninen, "Analysis of Capacity and Scalability of the LoRa Low Power Wide Area Network Technology," *European Wireless 2016; 22th European Wireless Conference; Proceedings of,* pp. 1-6, 2016.

[5] "Semtech LoRa Modulation Basics," May 2015. [Online]. Available: http://www.semtech.com/wireless-rf/lora.html

[6] Semtech Corporation, "Semtech SX1272 Datasheet," March 2015. [Online].Available: http://www.semtech.com/images/datasheet/sx1272.pdf.

[7] J. Petajajarvi, K. Mikhaylov, A. Roivainen, T. Hanninen and M. Pettissalo, "On the coverage of LPWANs: range evaluation and channel attenuation model for LoRa technology," in *ITS Telecommunications (ITST), 2015 14th International Conference on*, 2015.

[8] S. Hosseinzadeh, "Mathworks File Exchange," Jan 2017. [Online]. Available: http://uk.mathworks.com/matlabcentral/fileexchange/61340-multi-wall--cost231----free-space-signal-propagation-models

[9] "Propagation data and prediction methods for the planning of indoor radio communication systems and the radio local area networks in the

frequency range 900 mhz to 100 ghz," Recommendation ITU-R P.1238-8, 2015.

[10] COST Action 231: Digital Mobile Radio Towards Future Generation Systems: Final Report, 1999.

[11] A. G. M. Lima and L. F. Menezes, "Motley-Keenan model adjusted to the thickness of the wall," in *SBMO/IEEE MTT-S International Conference on Microwave and Optoelectronics, 2005.*, 2005.

[12] J. E. Bresenham, "Algorithm for computer control of a digital plotter," *IBM Systems Journal,* vol. 4, no. 1, pp. 25-30, 1965.

[13] J. W. McKown and R. L. Hamilton, "Ray tracing as a design tool for radio networks," *IEEE Network,* vol. 5, pp. 27-30, 1991.

[14] T. Holt, K. Pahlavan and J.-F. Lee, "A graphical indoor radio channel simulator using 2D ray tracing," in *Personal, Indoor and Mobile Radio Communications, 1992. Proceedings, PIMRC'92., Third IEEE International Symposium on*, 1992.

[15] S. Y. Seidel and T. S. Rappaport, "A ray tracing technique to predict path loss and delay spread inside buildings," in *Global Telecommunications Conference, 1992. Conference Record., GLOBECOM'92. Communication for Global Users., IEEE*, 1992.

[16] R. Valenzuela, "A ray tracing approach to predicting indoor wireless transmission," in *Vehicular Technology Conference, 1993., 43rd IEEE*, 1993.

[17] F. Villanese, W. Scanlon, N. Evans and E. Gambi, "Hybrid image/ray-shooting UHF radio propagation predictor for populated indoor environments," *Electronics Letters,* vol. 35, pp. 1804-1805, 1999.

[18] C. F. Yang, B. C. Wu, C. J. Ko, "A ray-tracing method for modeling indoor wave propagation and penetration," *IEEE transactions on Antennas and Propagation,* vol. 46, pp. 907-919, 1998.

[19] M. Ganley, R. Hartless, R. Rudd, K. Craig. , "Building Materials and Propagation Final Report," Ofcom, 2014.

[20] A. Asp, Y. Sydorov, M. Valkama and J. Niemelä, "Radio signal propagation and attenuation measurements for modern residential buildings," in *2012 IEEE Globecom Workshops*, 2012.